[1]**Maithem Alhussani**
maythem.hk@gmail.com
[2] **Mohsen Saniei**
m.saniei@scu.ac.ir
3 **Mortazavi _ S**
mortazavi_s@scu.ac.ir

# Improvement of the Transient Stability of Grid Connected Microgrids Including Inverter Based DGs Using DSTATCOM

Journal of Electrical Systems

***Abstract:*** - Microgrids are becoming popular because they can meet the needs of people who want energy from natural sources and are using more and more energy. Itis important to emphasis on numerous safety and control features of a microgrid. During the change from following the grid to forming the grid, the instability of frequency and voltage due to control problems becomes the main concern. Then, the paper uses a method to control the frequency and voltage of power generators so they can share power efficiently. Furthermore, we are suggesting a way to handle situations when there is not enough control and to keep the system strong. We are proposing a method to prioritize and shed different parts of the system in three stages to help with this. The effectiveness of the method depends on how quickly the system reacts and is calculated based on the changing speed of the frequency. The process combines the battery capacity system and D-STATCOM in the microgrid to provide a reliable power supply to customers for a long time without sudden power cuts. We test the proposed procedures on a smaller version of an IEEE 13-bus microgrid using MATLAB. We recreate the time-domain to see if the procedures work well.

AVR: Automated voltage regulator; BES: Battery energy storage; DG: Distributed generators; DSTATCOM: Distributed static compensator; ESS: Energy storage system; MPPT: Maximum power point tracking; PCC: Point of common coupling; PI: Proportionalintegral; PV: Photovoltaic; ROD: Rate of discharge; SOC: State of charge; SPWM: Sinusoidal pulse width modulator.

## I. INTRODUCTION

Using natural energy sources with companies that provide electricity has been a good way to meet the need for environmentally friendly power without any breaks.. As a result, adding and Putting together small power sources with the main power companies is a great way to make small and mediumsized microgrids. Because the DGs in the regular microgrid work the same way, any disruptions and power to be shared are spread out evenly so that no DG gets overloaded. The voltage and frequency where the microgrid connects to the utility have a lot of changes. However, with more research, microgrids are better able to combine different types of power sources, such as synchronous machines Power sources include batteries, solar panels, and inverters. Using powerful synchronized machines with high inertia in a microgrid system that lacks inertia helps the system to stay stable during sudden changes. When something goes wrong in the microgrid system, it becomes difficult to share the power properly. The inactivity less inverter founded DG can quickly adjust the voltage to meet the power needs. On the other hand, the fast power changes don't work well for high inertia DG (synchronous machine). Furthermore, the problem becomes serious when the power generation of the DG decreases a lot because of the weather. [4]. So, when we have power sources that take a long time to start and ones that start quickly, it makes it hard to keep everything running smoothly. To fix these problems, we use a powersharing plan with load shedding to make things work better of the microgrid [5, 6]. Please rewrite this text using easier words. A method to control frequency using droop and to reduce the load.The plan in [5] is studied to keep an independent small power grid stable. Many researchers have suggested different ways to keep the electric system stable by reducing the load when the frequency drops. The usual UFLS technique works by cutting off a set amount of power usage when the frequency reaches certain limits. This traditional plan uses a way of testing different choices until they figure out the correct amount of weight to be removed. The plan has a problem because it either causes too much or too little weight loss to keep the system stable. By taking a certain amount of electricity from the right place, it helps the UFLS system adapt. The smart way to reduce electricity use measures how the power changes as time passes.Therefore, the weight is decreased according to the lack of power at each stage. A lot of research has been done on adaptive methods for UFLS. A study comparing traditional, partially adjustable, and fully adjustable UFLS systems. is

[1] * Correspondence: Maythem.hk@gmail.com
[1]Electrical Engineering Department, shahid chamran University of Ahvaz

shown in reference [12]. The flexible stack shedding plot shows how the frequency changes and the strength of the disturbance causes the stack to be shed. Help to make shedding strategy better, [13, 15] use the voltage of the stack to shed the loads. "In the range of 16 to 17, we check how much the recurrence deviates according to the dormancy constant, and we follow a pattern of reactionbased event approach. " The method suggested in [18] makes the shed ding happen where the voltage decrease and the frequency change are the highest. The authors use numbers and genetic calculations in the process of stack shedding in their research. Furthermore, some smartgrid techniques for reducing power usage are discussed by [21, 22]. The plans suggested so far need to be studied more to make a microgrid work better. The microgrid system has many different power sources, batteries, and things that use power. This makes it hard to figure out exactly when to cut off power to certain things. Also, a small problem in a standalone microgrid can make the system unstable. A lack of reactive power during automatic operation can cause the system's voltage to drop. Afterwards, the drop in voltage changes how much power the load uses. Therefore, if the frequency and its change are measured late, the plan to reduce power usage may not be accurate because the estimated amount of power needed will be less than what is actually needed. Also, another problem with this plan is that the amount of load shed does not directly match The UFLS scheme needs more power. To make it better at handling sudden changes, we are adding things like ultracapacitors to help support the frequency. by [23]. Further to adjust for changes in speed until the governor starts working, the superconducting storage devices are implemented by [24]. The powerful magnetic device stores energy to help keep the power system stable during sudden changes, and it also helps reduce the amount of power being used in [25]. However, it's difficult to make Quick storage devices work within a specific speed and can recover energy. Additionally, we haven't planned to use slow storage devices in the microgrid when we designed the UFLS. The energy storage system is really important for the microgrid. Adding a storage system helps to manage fluctuations in power and equalize differences in power.. Additionally, the storage system helps make the microgrid (which mostly uses renewable energy) more reliable and stable. Adding it could make it cheaper to improve the power lines and infrastructure to keep up with the growing need for electricity. So, a battery is added to the microgrid to help when there's not enough power. The BES system helps with power cuts so that local power needs can still be met.

However, using battery storage devices may not always give strong and quick support because these devices don't store a lot of power for their size. While these storage devices make the microgrid more resistant to change, they don't work well during sudden changes. In simpler terms, the microgrid doesn't have enough strength to handle sudden changes in the power system. A lot of focus has been on using DSTATCOM in microgrids Please rewrite this text in simpler terms. DSTATCOMs only work to make sure the power system is balanced and has a good power factor. Adding DSTATCOMs to the distribution system has caught the attention of many people because it can adjust the voltage at the point of common coupling or the current in the line. This paper explains how the DSTATCOM can settle issues with control sharing between two sorts of DG by changing the voltage. The article moreover notices that the DSTATCOM and the tall inactivity framework can offer assistance keep the framework steady for a small whereas some time recently diminishing the power utilization starts. This manuscript suggests a plan to turn off some power sources during high demand and share power between different generators. In the organization of microgrids, secondary control is about sharing power and reducing the amount of electricity used. The paper uses a self adjusting technique Using strategy that combines proportional and integral control, while also sharing power. The plan uses different technologies to control the voltage and frequency of the microgrid, including highinertia DGs, battery storage, and a monitoring system called DSTAT COM. However, a lot of attention has been given to a situation where there is more demand for electricity than there is supply. So, to handle this situation, we suggest using a three stage plan for cutting power that is not dependent on a specific system and gives priority to certain tasks. The plan includes three steps of cutting power and also takes into account a system for storing energy. The fast acting DSTATCOM helps with quick power issues and the slow battery energy storage systems help maintain power stability for a while. So, the important points of the suggested work are:

- A nitty gritty examination of a Pf and QV hang control methodology to accomplish an productive power distribution between the diverse inertial DGs.The manuscript suggests a way to manage power outages by giving priority to certain things and adjusting as needed.
- To make the system more stable, we carefully check how well the battery and DSTATCOM in the microgrid are working when we use the load shedding algorithm.
- The manuscript is arranged like this: Unit II presents the test system used. Unit III explains how the controller is designed for each power source in the microgrid. The suggested way of controlling something

## II. MICROGRID STRUCTURE

This study looks at a threephase 13 transport microgrid system, which is shown in the picture. When you rewrite this text in simple words, please provide the text you would like to have simplified. Then, I can help you rephrase it in a simpler way. The small test framework includes a solar power source, a synchronous machine, and some controllable loads. The small electrical system will control how much battery power is used and spread it out evenly. The capacity framework can be flexible. They are organized so that we can examine their features in a shorter amount of time. In realtime situations, the framework evaluations can be adjusted. The system settings are shown in the back of the book. The microgrid is 8200 feet long. Rewrite this in simple words: the extent or measurement of something from end to end. The microgrid is connected to the power company through a special transformer. The Simulink platform in MATLAB 2021b is used to copy and test the planned microgrid system. Times is specified, Times Roman or Times New Roman may be used. If neither is available on your word processor, please use the font closest in appearance to Times. Avoid using bit-mapped fonts if possible. True-Type 1 or Open Type fonts are preferred. Please embed symbol fonts, as well, for math, etc.

## III. POWER SOURCE CONTROL

### *A. Micro Source*

The sketched out inactivity less inverter founded photovoltaic system makes a most extraordinary of 100 kW at 1000 W/ m2 sun based irradiance. MPPT uses Incremental Conductance for better control.

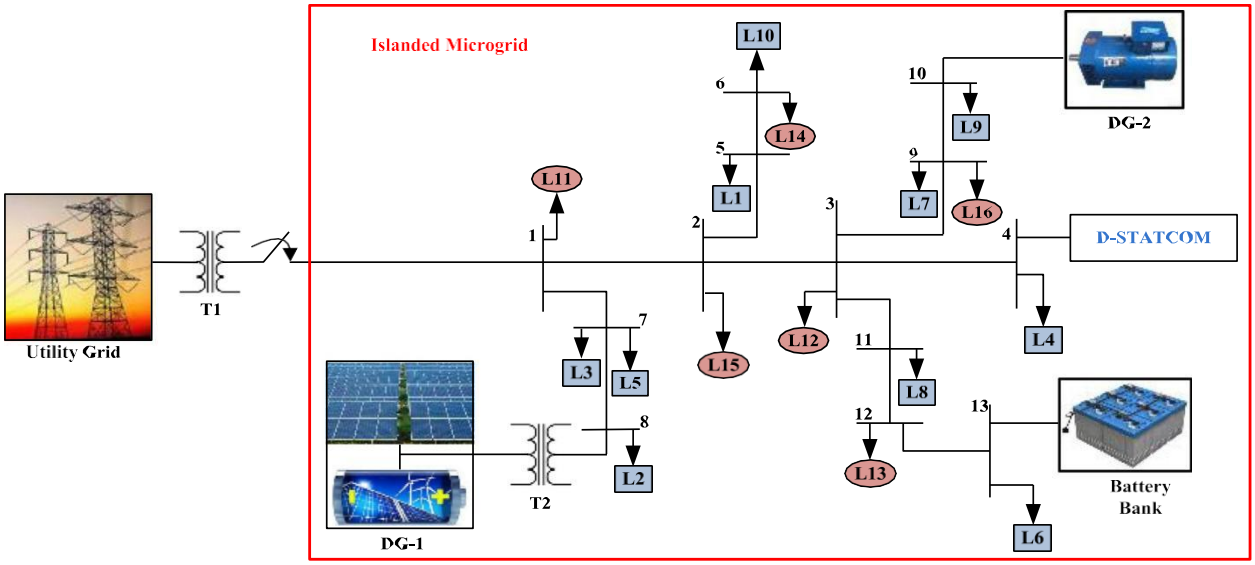


Fig. 1 study system

Rewrite this text using simpler words. The MPPT controls how often the power is turned on and off based on the required voltage to get the most power[30]. The DCAC inverter changes most DC power it can get into AC power by a governor system founded on a certain position edge. The governor changes the voltage in the power supply based on the voltage changes at the point of common coupling. The power taken from the solar panel system goes to the DC link[31]. So, the $V_{dc}$ In power factor, the reference current for reactive power (Iqref) is assumed to be zero. In addition, the governor system uses phase locked loop to keep the system in sync

Rotor angular velocity is different from the stator angular velocity. Applying dq0 transformation [29], stator voltage equations can be written as:

$$\frac{d}{dt} i_{DG-1} = \frac{-R_f}{L_f} i_{DG-1} + \frac{1}{L_f} [v_{DG-1} - v_{PCC}] \quad (1)$$

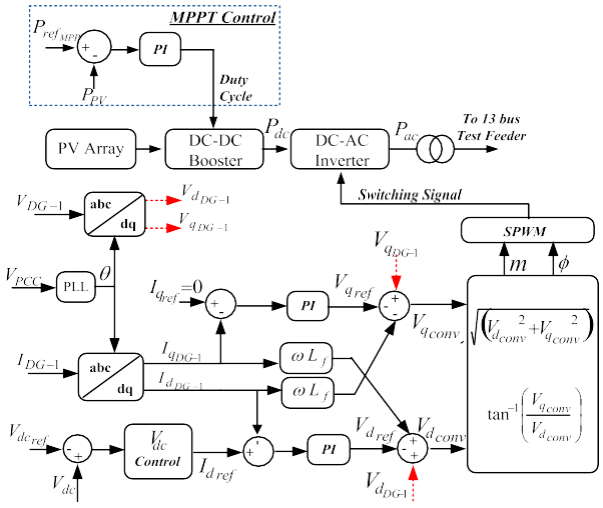


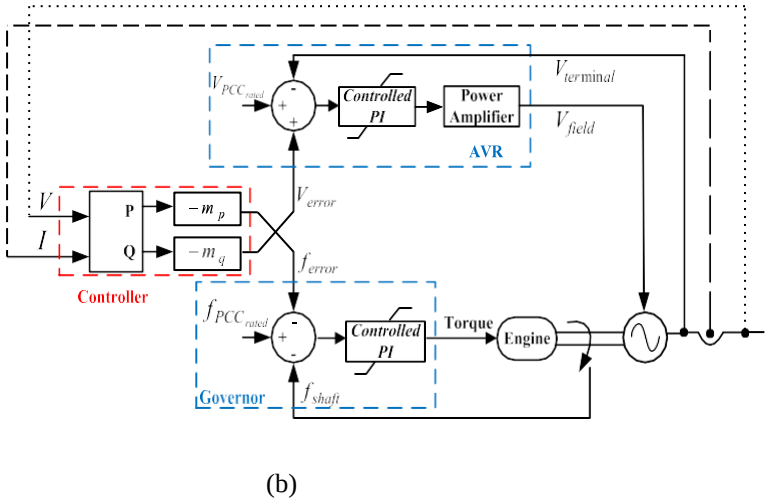


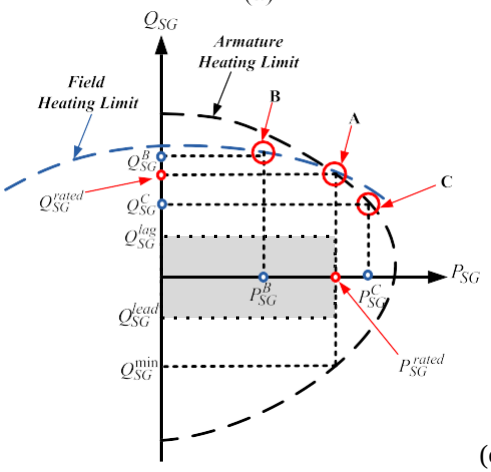


Fig.2Controller made for DPG. **a** Inverter based generators that produce power in different locations **b** The management of generators that produce power at the same time **c** A graph showing the ability of synchronous generators to produce power

On using the Park's transformation on (1) to transform it into the rotating reference frame, the equation is reframed as:

$$\frac{d}{dt}\begin{bmatrix} i_{d_{DG-1}} \\ i_{q_{DG-1}} \end{bmatrix} = \begin{bmatrix} \frac{-R_f}{L_f} & 0 \\ 0 & \frac{-R_f}{L_f} \end{bmatrix} \begin{bmatrix} i_{d_{DG-1}} \\ i_{q_{DG-1}} \end{bmatrix} + \frac{1}{L_f}\begin{bmatrix} v_{dconv} \\ v_{qconv} \end{bmatrix} \quad (2)$$

where,

$$v_{dconv} = v_{d_{DG-1}} - v_{d_{PCC}} + \omega L_f i_{q_{DG-1}}$$

$$v_{qconv} = v_{q_{DG-1}} - v_{q_{PCC}} - \omega L_f i_{d_{DG-1}} \quad (3)$$

Using the terms Vdconv and Vqconv, the magnitude and the angle for the SPWM are generated. Hence, the inverter's switching pattern as (4)

$$\phi = \tan^{-1}\left(v_{qconv} / v_{dconv}\right)$$
$$m = \sqrt{v_{d_{conv}}^2 + v_{q_{conv}}^2}$$

(4)

The major advantages of using a current-control strategy can be stated as: 1) It provides protection against the over-current. 2) It reduces the contribution of fault currents by the unit. 3) It limits the converter output current during fault conditions

On the other hand, the design of a high inertia synchronous system regulates the voltage and the frequency by a different approach. The frequency of the generator is regulated by adjusting the torque on the basis of speed error. Simultaneously the reference speed is adjusted according to the active power measured. Further, the automated voltage regulator (AVR) integral action regulates the voltage when the voltage reference error becomes zero [33]. The control strategy of the generator is presented in Fig. 2b

### *B. D-STATCOM*

D-STATCOM is a shunt connect voltage source converter (VSC) in the distributed power system. The integration of D-STATCOM in the power system is the most effective solution for reactive power compensation. A sudden change in reactive power demand or supply cannot be compensated by a synchronous machine, as fast as the voltage source converter [36]. It regulates the line voltage to control the leading or the lagging reactive power in the system with a response speed of 1-2 cycles [37]. Thus, the compensating device helps to regulate the voltage within its rated limit by efficient power management. In a grid-connected microgrid, the voltage fluctuations are majorly detected at the load end of the feeder. However, it is not possible to detect the voltage drop and the compensation point in an islanded microgrid. Therefore, the designed D-STATCOM is interconnected in the microgrid with the bus having critical loads. Figure 3 presents the schematic layout of the reactive power compensating D-STATCOM connected to the critical load. The major role of D-STATCOM is to perform a conversion of input DC voltage to an output three-phase AC voltage. The instantaneous input and output power have to be balanced properly. Therefore, the input terminal of VSC is connected to a capacitor, which acts as a passive voltage source. On the other hand, the output of the VSC is connected to a coupling transformer, which acts as a passive current source. The output current fed by the D-STATCOM can be expressed as in (5)

$$I_{stat} = \frac{V_{stat} - E}{X}$$

(5)

Here, Vstat and E represent the voltage at D-STAT COM and bus respectively, X signifies the system reactance and Istat presents the current fed by the D-STATCOM. On using eq.(5), the reactive power compensated by the D-STATCOM can be stated as

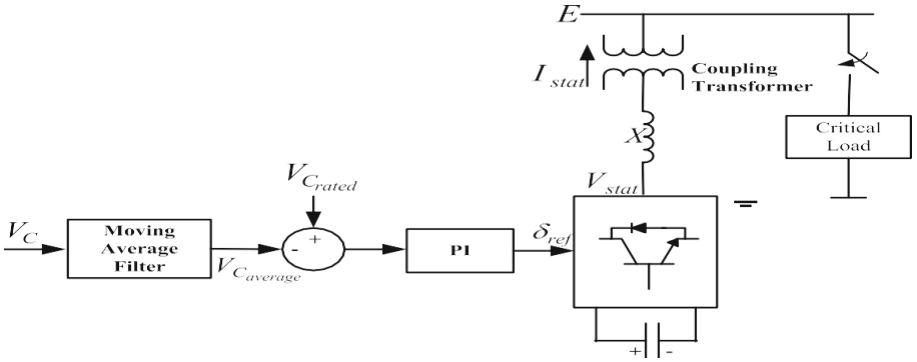


Fig. 3 Controller design for D-STATCOM

$$Q_{stat} = \frac{1 - \left(\frac{E}{V_{stat}}\right)}{X} V_{stat}^2$$

(6)

Analyzing (6), it can be clearly stated that the voltage fed by the D-STATCOM regulates the reactive power of the system [38]. The control over reactive power is attained by keeping the D-STATCOM voltage in phase with the system voltage. Moreover, these in phase voltages do not allow the charged capacitor to supply active power into the system. Further, at zero frequency of the DC capacitor, the reactive power of D-STATCOM is zero. Thus, it can be concluded that the DC capacitor does not play a role in reactive power generation. It proves that the VSC of D-STATCOM is capable of facilitating the free flow of reactive power among the three AC terminals [39]. The DC capacitor only enables the compensation for the instantaneous power mismatch in the system.

### C. *Storage device*

The storage system considered in this study is the Lithium-Ion battery model acquired from the Matlab SimPowerSystems library. The battery parameters are set to support the P-f and Q-V control within the system. In-depth analysis regarding the storage devices presented in [40]. Due to the uncertain fluctuations in renewable power generation and load demands, lithium-ion batteries are highly preferable in microgrids. This is due to the fact that these batteries can be exploited up to their maximum capacity [41]. Therefore, to achieve a deep cycle operation, the lithium-ion batteries have been modelled with the proper selection of parameters. The voltage of a completely charged Li-Ion battery (i.e., Ebattery) can be expressed as:

$$E_{battery} = E_0 - K\frac{Q}{Q_{actual} - 0.1*Q} \cdot \left(i_{filtered}\right) - K\frac{Q}{Q - Q_{actual}} \cdot \left(Q_{actual}\right) + A\ \exp\left(-B.Q_{actual}\right) \tag{7}$$

The analytical battery model can be presented by (8) and (9) for charging and discharging respectively.

### D. *Charge*

$$V_{battery} = E_0 - R_{\text{int}} \cdot I_{battery} - K\frac{Q}{Q_{actual} - 0.1*Q} \cdot \left(i_{filtered}\right) - K\frac{Q}{Q - Q_{actual}} \cdot \left(Q_{actual}\right) + A\ \exp\left(-B.Q_{actual}\right) \tag{8}$$

### E. *Discgarge*

$$V_{battery} = E_0 - R_{\text{int}} \cdot I_{battery} - K\frac{Q}{Q - Q_{actual}} \cdot \left(Q_{actual} + i_{filtered}\right) + A\ \exp\left(-B.Q_{actual}\right) \tag{9}$$

where, Vbattery and Ibattery represent the battery voltage and current respectively. K signifies the polarization constant and Rint signifies the internal battery resistance. The battery capacity is represented by Q whereas the actual charge of the battery is presented by Qactual. The constant voltage and the filtered current of the battery are stated as E0 and filtered respectively. To address the exponential zone of amplitude and time constant inverse, under the characteristic curve of the battery are termed as A and B respectively [42].

## IV. PROPOSED CONTROL METHOD FOR MICROGRID

In order to attain a balanced voltage profile and a reduced system loss, efficient power-sharing is crucial. Power-sharing can be controlled either by implementing a communication based centralized control strategy or by decentralized droop strategy. In recent times, communication strategies are avoided because of their economic limitations. Moreover, the interruptions and break-down in communication are few added up limitations to the communication-based control strategy. Hence, decentralized droop control strategies have drawn major attention. The droop control facilitates faster stability and an efficient power-sharing among

the distributed generations in a microgrid. The droop strategy can be explained using the basic circuit of two AC sources (i.e., V1 ∠ δ and V2 ∠ 0) connected by reactance (X) dominated impedance line. The power transfer between the two sources can be termed as:

$$P = \frac{V_1 V_2 Sin\delta}{X}$$

$$Q = \frac{V_1^2 - V_1 V_2 Cos\delta}{X} \tag{10}$$

It can be analyzed that the active power transferred is in proportion to δ, as the angle tends to be small during the normal operation of the system. The reactive power transferred also varies proportionally with the difference between the voltage magnitudes at the two ends [43]. Thus, the droop characteristics can be framed as in (11) and (12), and are graphically shown in Fig. 4.

$$\omega = \omega_{max} - m_p P$$
$$\Rightarrow m_p = \frac{\omega_{max} - \omega_{min}}{P_{max}} \tag{11}$$

$$V = V_o - n_q Q$$
$$\Rightarrow n_q = \frac{V_{max} - V_{min}}{2Q_{max}} \tag{12}$$

Therefore, the control strategy of DGs present in an inductance-dominated microgrid implements active power-frequency (P-f) and reactive power-voltage (Q-V) droop control characteristics [44]. The strategy aims to maintain the voltage and the frequency of the microgrid within its limit, along with a precise power-sharing between the multiple power generators present in the microgrid. As the grid-forming microgrid possesses minimum inertial stability, it becomes highly sensitive to the dynamic load demand. This sensitivity increases the system instability with the increment in the frequency deviation. Therefore, in the second and third stages of the proposed load shedding algorithm, it has been observed that the operating frequency tends to maintain the nominal frequency (60 Hz). Thus, to reach the predetermined operating value of the system frequency, the second stage of load shedding strategy triggers and sheds small load in iterative steps. Subsequently, the third stage of load shedding tends the difference between the operating.

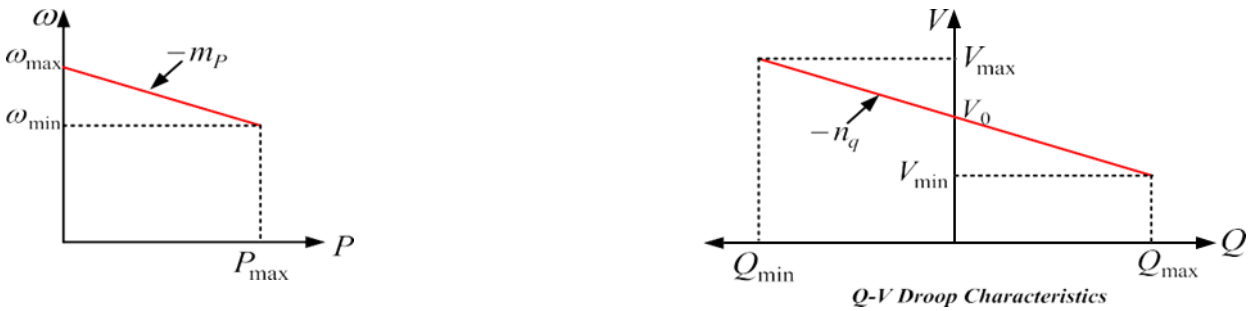


Fig. 4 Droop characteristics for power-sharing

frequency and the nominal frequency to approximately zero by shedding the very small loads. The algorithm for the proposed load shedding scheme is presented in Fig. 6 and each shedding stage is analyzed in the section as follows:

*A. Proposed load shed amount*

Stage-I, stage-II, and stage-III of the load shedding scheme shed the load by measuring the frequency, the rate-of-change-of-frequency and Δf respectively. However, the amount of shed load differs in each stage. The proposed scheme ensures an iterative shedding process and the sheddable loads from busses are decided using the strategy presented in [45]. The iteration continues until it satisfies the individual criterion. The scheme computes the shedding amount concerning the instantaneous rate of change of frequency measured. From Fig. 5 it can be observed that the rate-of-change-of-frequency varies significantly during the transition between the stages. The load to be shed during an iteration is computed using (14).

$$P_{Load-shed} = K * abs\left(\frac{df}{dt}\right) \tag{13}$$

where,

$$K = \frac{2 * H_{equivalent}}{f_{rated}} \tag{14}$$

Here, PLoad − shed is the amount of load shed in each iteration, and K denotes the shedding constant obtained from the swing equation of the system. Equivalent denotes the normalized inertia constant. It can be observed from Fig. 5 that the rate-of change-of-frequency at PCC is significantly high and it is a directly dependent factor of the power deficit.

At the occurrence of an islanding instant, the significant difference in rate-of-change-of-frequency occurs due to the reduced moment of inertia of the gridforming microgrid. As a result, the amount of load shed is directly proportional to the frequency derivative. Further, Fig. 5 illustrates that, with every step of load shed, the rate-of-change-of-frequency reduces with reducing power deficit and tends to attain approximately zero. Thus on realizing eq.(14), it can be analyzed that with the decrease of rate-of-change-offrequency, the amount of load shed decreases. Therefore, this strategy of shedding the load amount in the proposed load shedding scheme presented in Fig. 6 helps to shed the proportional amount of load concerning the power deficit

*B. Battery and DSTATCOM performance simultaneously with the proposed load shedding strategy*

The presence of a storage system in a microgrid adds to the advantages of the proposed load shedding strategy. It provides a certain amount of power to the extra loads by a certain period of time. The battery storage element supports during the islanded microgrid and compensates for the steady part of the power deficit. Conversely, the D-STATCOM compensates the system disturbances during the transients. The batteries supply a steady power at a specified nominal rate of discharge (RoD1) till they reach 50% and at RoD2 till they reach 30% of their state-of-charge (SoC). The SoC of a battery is a timescaled factor with respect to the rate of power delivery. In other words, the instantaneous change in power supply does not change the SoC instantaneously. Therefore, considering the deep discharge limit of the battery, the power supplied by the battery is intentionally reduced to RoD2 at a specified SoC condition of 50%. It can be observed from Fig. 6 that the algorithm clearly shows the operational performance of the storage device.

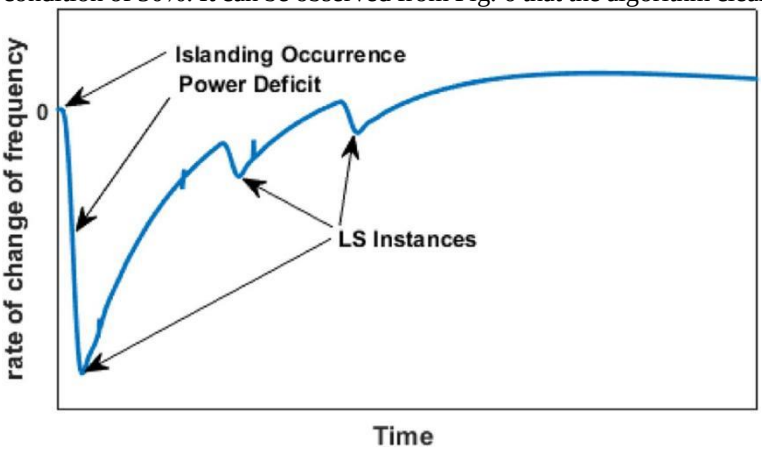


Fig. 5 Response of rate-of-change-of-frequency with respect to the power deficit

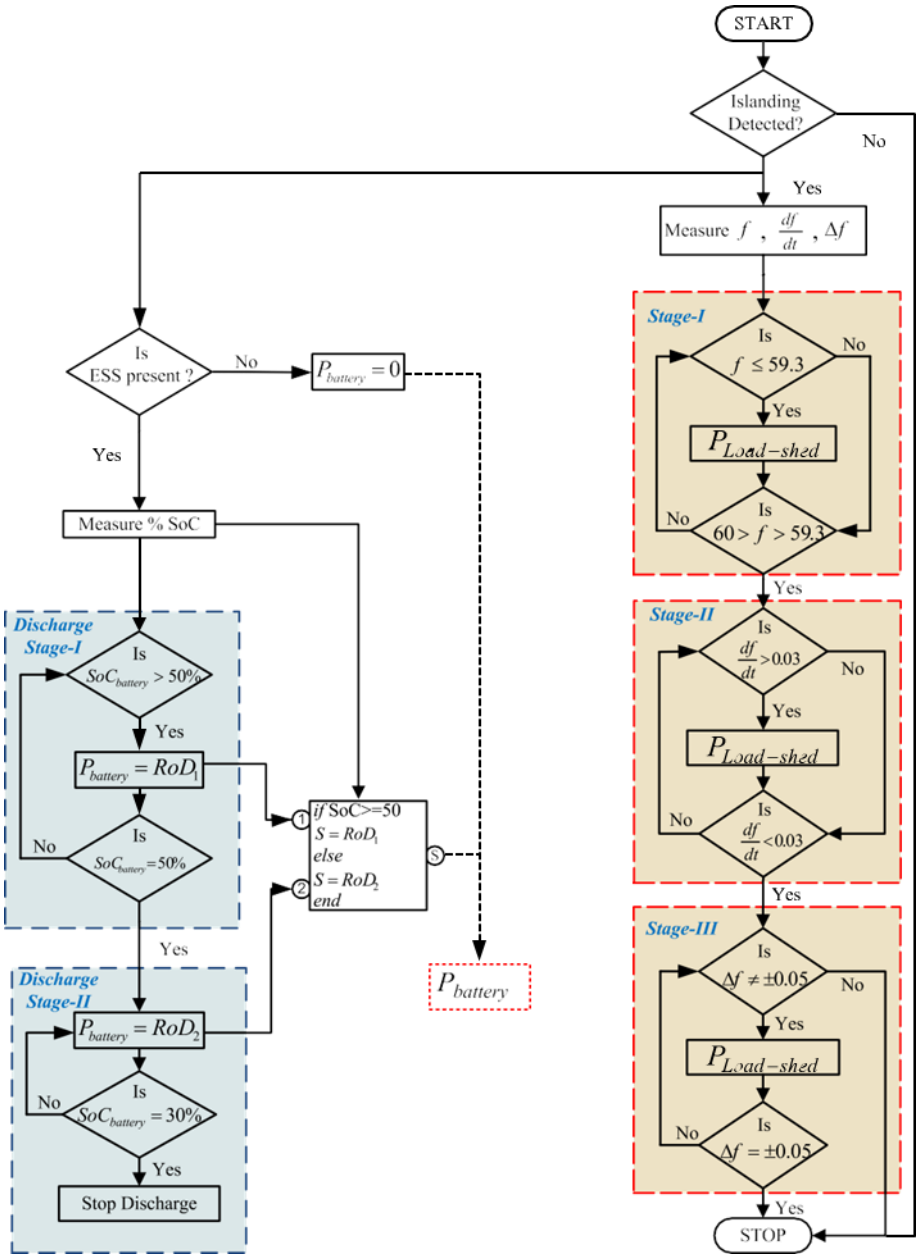


Fig. 6 Proposed load shedding algorithm

*C. Stage-I of load shedding*

The first stage of the proposed load shedding scheme functions with the objective to hold back the normal operating conditions of the microgrid after facing a severe power deficit. In Fig. 6, load shedding steps involved in each stage are highlighted. From the conventional strategy of power networks, it is observed that the rate of decrement of the frequency inversely depends on the cumulative short-circuit MVA of the entire integrated system [46]. However, in the microgrid the short-circuit MVA dramatically falls down due to the power electronic interfaces present in the system. Therefore, the microgrid fails to withstand the extra load demand. As a result, at the instant of islanding, system frequency drops down in proportion to the surplus load demand. The analyzed microgrid characteristic can be observed in Fig. 5. From Fig. 5 it can be clearly observed that the rate-of-change-offrequency is proportional to the microgrid demand. So, to regain the rate-of-change-of-frequency, a large load is shed using eq.(14) in an iterative process. Thus, the load shedding starts when the system frequency goes beyond 59.3 Hz. The iterative process continues until the frequency regains to the giventhreshold set value f ≥ 59.3. The instant, when the microgrid reaches the set frequency limit for operational stability, the stage-II triggers

*D. Stage-II of load shedding*

The loads in this stage are shed by considering the rateof-change-of-frequency(df\dt). Smaller values of load shed in each step tends the frequency towards the operating nominal frequency of 60 Hz. The proposed algorithm in Fig. 6 illustrates that the iterative shedding

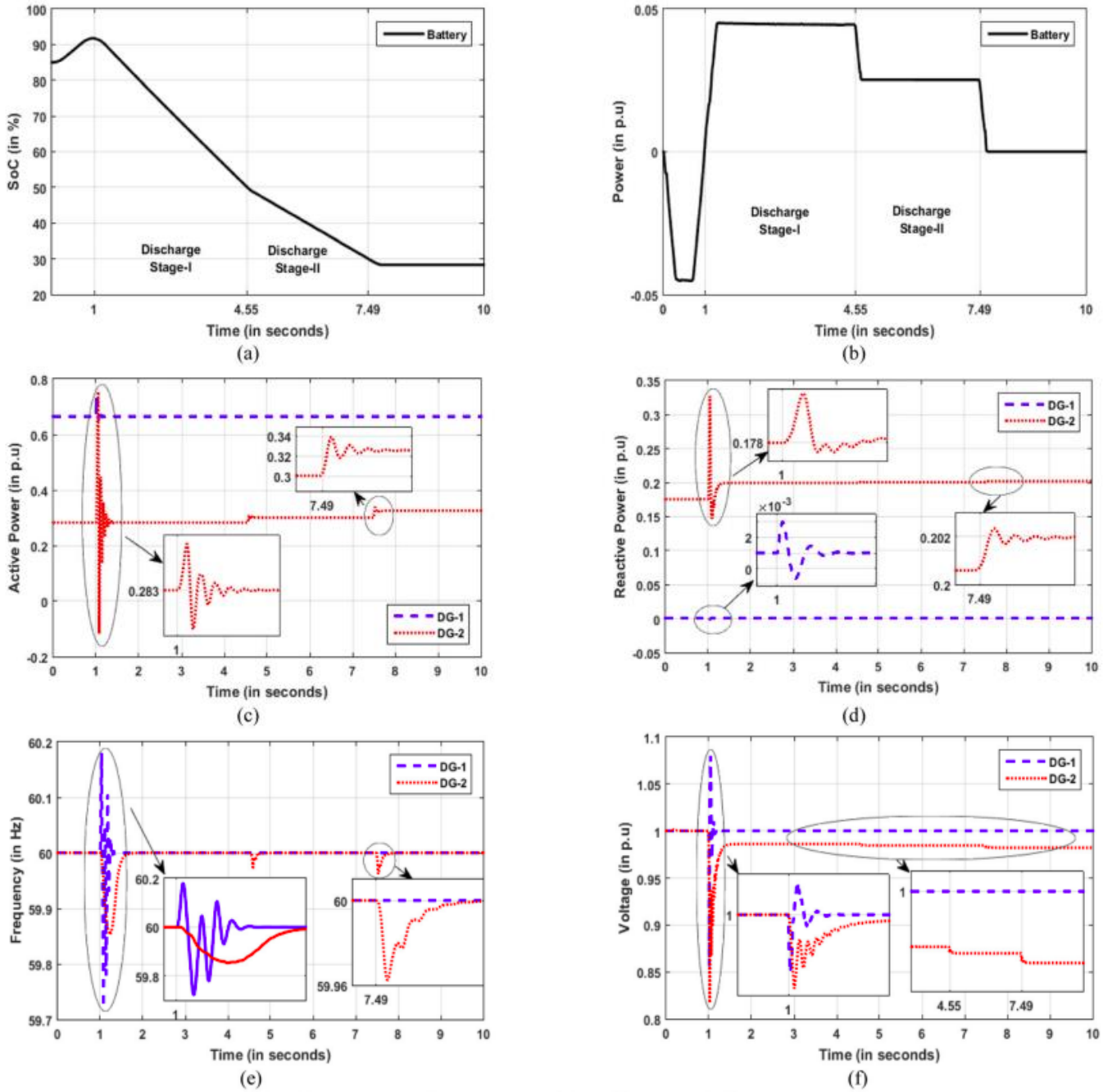


Fig. 7 Battery performance and its effects on DG parameters (a) Battery's state of charge, (b) Battery power, (c) Active power fed by the DGs, (d) Reactive power fed by the DGs, (e) Frequency variation in DGs, (f) Voltage variation in DGs

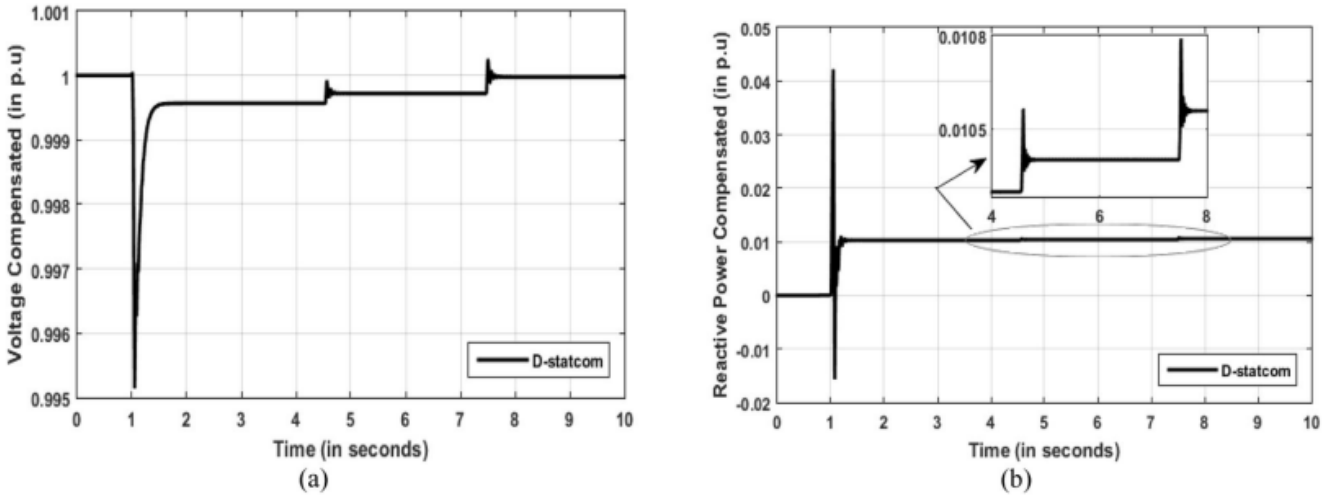


Fig. 8 D-STATCOM's performance (a) Voltage compensated, (b) Reactive power compensated

loads in a very small amount and makes the system stable. The stage reaches an end on achieving the Δf to be approximately zero. The amount of load shed in each iteration and in each stage of the algorithm is based on the absolute rate-of change-of-frequency of the microgrid. Hence, the shedding scheme is independent of the power generation. As a result, the climatic challenges or the operational challenges will not affect the load shedding strategy. Thus, the load shedding controls the microgrid to attain

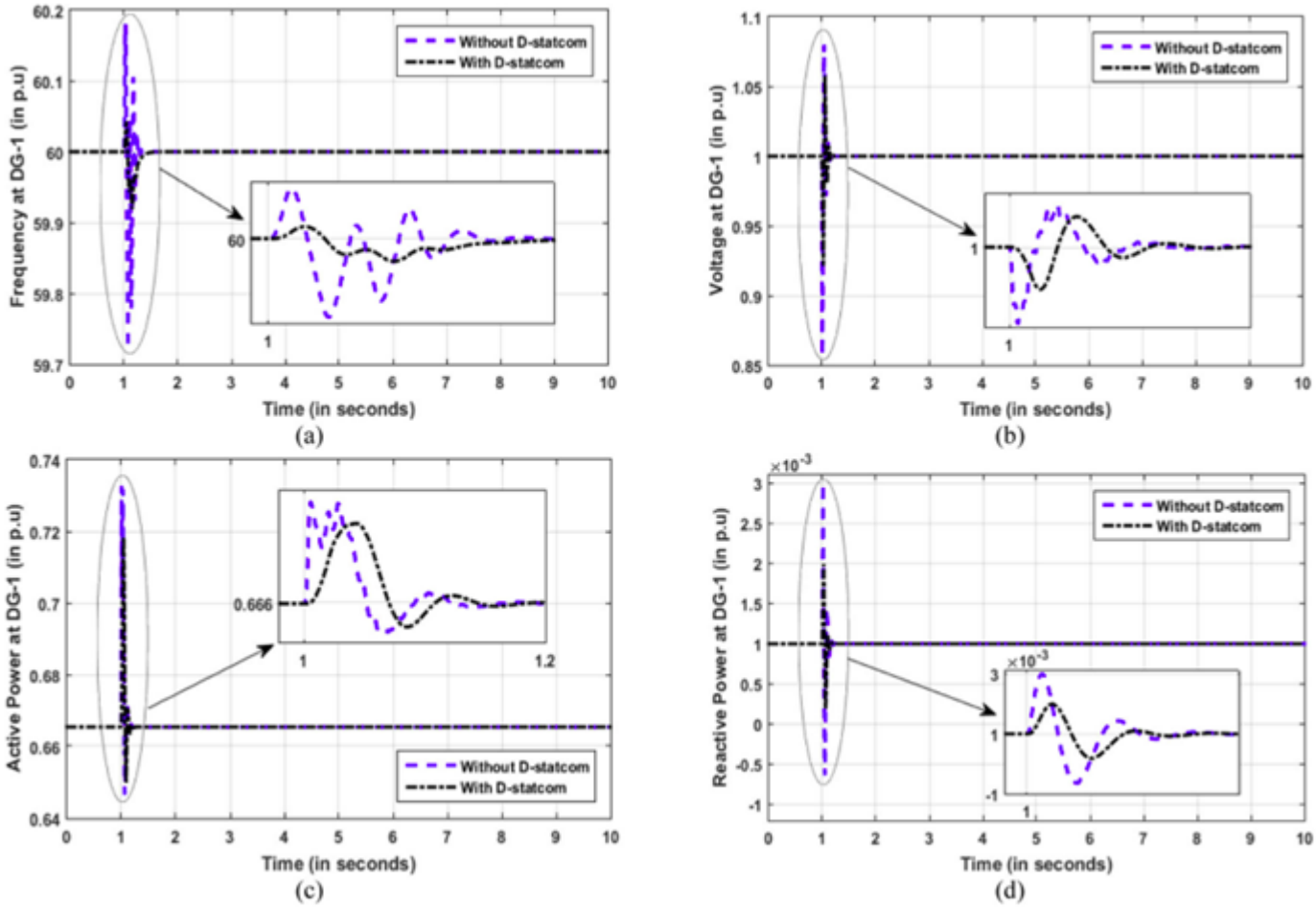


Fig. 9 Effects of D-STATCOM on the DG-1 parameters (a) Frequency, (b) Voltage, (c) Active power, (d) Reactive power

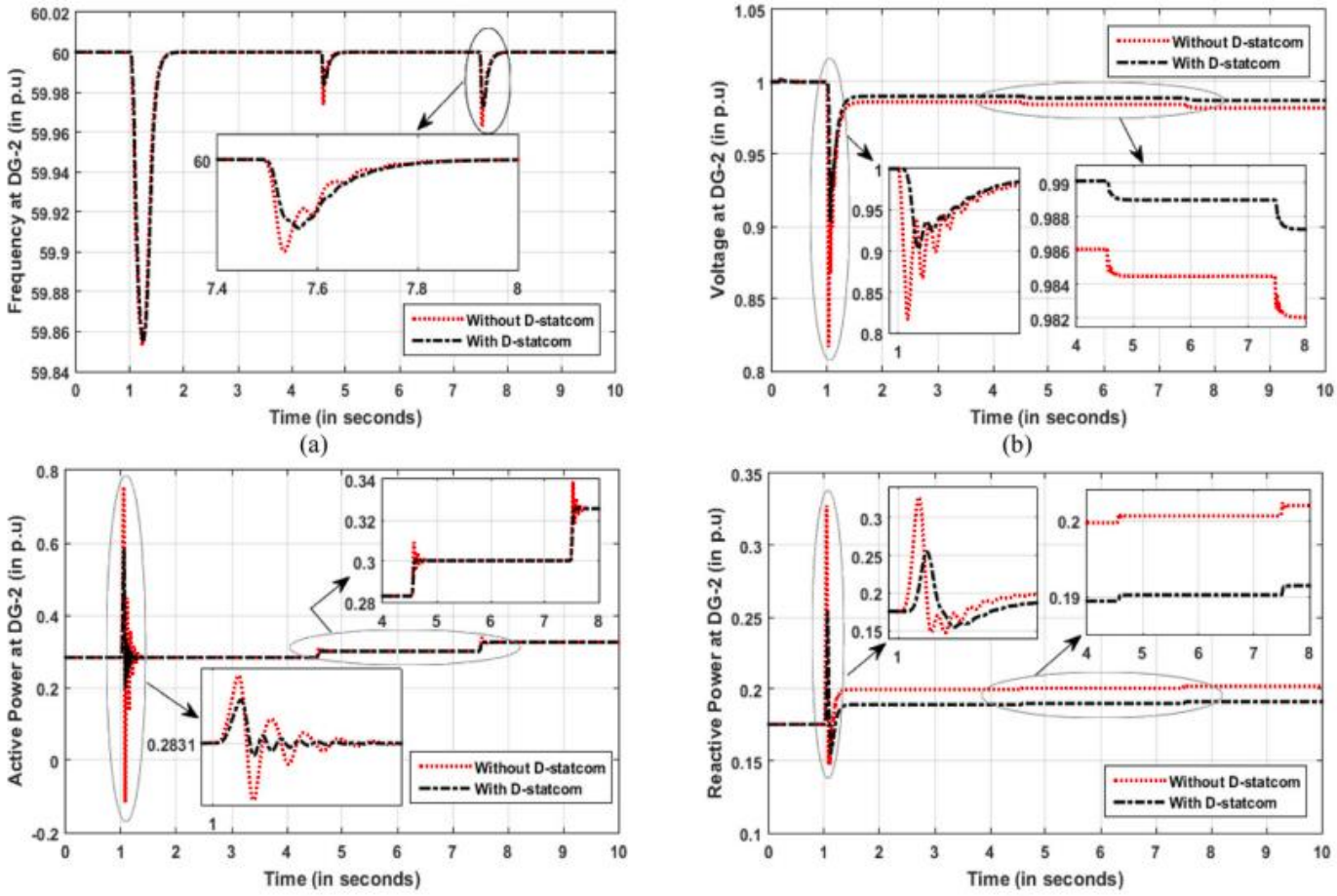


Fig. 10 Effects of D-STATCOM on the DG-2 parameters (a) Frequency, (b) Voltage, (c) Active power, (d) Reactive power

stability during the grid-forming mode of the microgrid. Further, the power-sharing scheme subsequent to load shedding strategy also operates to maintain a stiff system synchronization.

## V. RESULT ANALYSIS

This section presents the efficacy of the proposed approach under the system undertaken. About four different cases are simulated to analyze the performance of the system. Initially, the performance of the compensating devices present in the test system is analyzed individually and subsequently the proposed load shedding approach. Case-1 highlights the power-sharing performance within the microgrid integrated only with a battery storage device under 5% of overloading. Case-2 is an extension of the first case. It integrates D-STAT COM into the system and analyses its effect on the distributed generators present in the system. Highlighting the power-sharing strategy in Case-1 and Case-2, an emphasis has been given to investigate the power-sharing and load shedding strategy together in the subsequent cases. Case-3 verifies the system stability using load

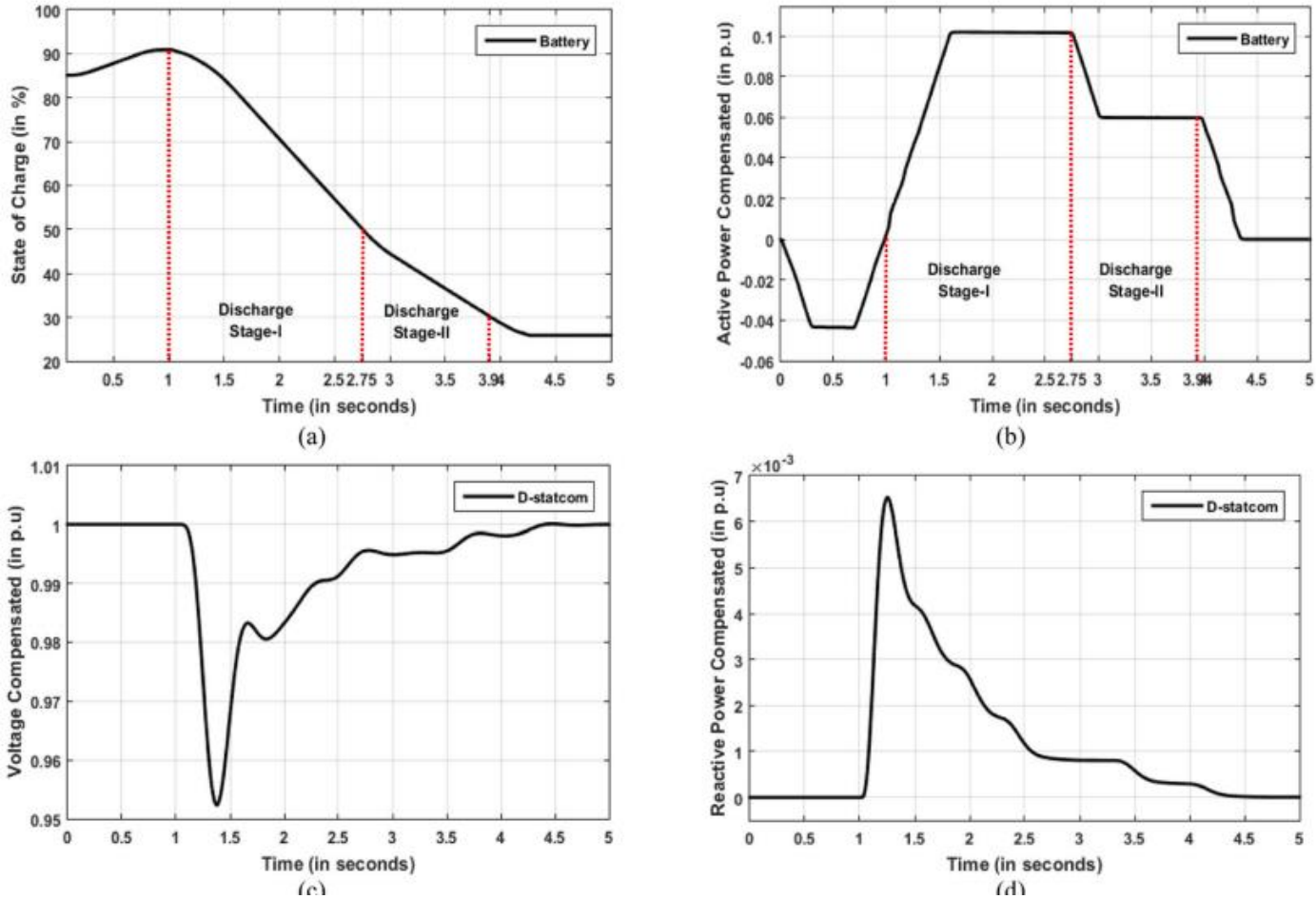


Fig. 11 Power compensated by the storage device and D-STATCOM (a) Battery's state of charge (b) Active power compensated by battery (c) Voltage compensated by DSTATCOM (d) Reactive power compensated by DSTATCOM

shedding strategy under 30% of active power and 10% of reactive power overloading condition. Further, in Case-4 the load shedding strategy is examined under a power deficit scenario, where the power generation at the DG end reduces significantly.

### *A. Case-1*

The case analyses the efficient power-sharing with the operating storage system present in the microgrid. The test system is formulated with 5% of overloading with the absence of D-STATCOM. It can be analyzed from SoC and battery power, that the battery charges itself while present in a grid-connected mode. On the detection of an islanding instance (i.e., 1 s), the battery system discharges itself as shown in Fig. 7a. Thus the battery power and the synchronous generator handles the small active and the reactive power overloading of 5%. At time 4.55 s, when the battery attains 50% of SoC, the power to be fed is reduced. On attaining the 30% of SoC at 7.49 s, the power fed by the battery is approximately zero. The active power fed by a battery based on the SoC can be studied in Fig. 7b. In the meantime, when the battery power reduces, the microgrid load demand is compensated by the synchronous generator of the microgrid. The photovoltaics do not increase its power generation as it is an MPPT based system and always supplies the maximum power in the system. The DG-2 increments the power in two steps at time 4.55 s and 7.49 s as illustrated in Fig. 7c. The reactive power fluctuations are negligible, as only the active power of the battery is compensated by the DG-2 in this case study. This negligible reactive power variation of DG-2 is presented in Fig. 7d. The increase in power generation by DG-2 is attained by reducing the DG voltage and frequency. Thus, the drop in voltage and frequency corresponding to the power increment can be analyzed from Fig. 7e and f respectively.

### *B. Case-2*

Case-2 is an extension of the case-1. The system is considered with a similar overloading condition of 5% with the integrated power sources, storage device and a DSTATCOM. The power-sharing is efficient in Case-1 but the reactive power overloading is solely controlled by the synchronous generator from the instance of islanding. In order to support the reactive power compensation, the D-STATCOM is integrated and its effect on the system is examined in Case-2. The D-STATCOM is assumed to be triggered at the detection of an autonomous mode of operation. The voltage control and reactive power compensated by the D-STATCOM can be examined through Fig. 8a and b respectively. It can be studied that with the reduction in battery power and an increase in synchronous generation, the D-STATCOM simultaneously increases the compensation level. Such that 60% of extra reactive power demand is fed by DG-2 and the remaining 40% of overloading is fed by the D-STATCOM. This helps in avoiding sudden stress on the synchronous generator to generate extra power beyond its generation limit. The presence of D-STATCOM has highly enhanced the transient stability of the system and has reduced the fluctuations in the system parameters during the steady-state operation. This

can be analyzed by considering a comparative study of the system responses with and without D-STATCOM. Figure 9a-d and Fig. 10a-d illustrates the effects of D-STATCOM on DG-1 and DG-2 respectively. Further, in a comparative approach, Table 1 highlights the suppression of peak overshoot and rise time during transient conditions. The table also emphasizes the enhancement of the settling time in both the DGs integrated with the microgrid. The integration of D-STATCOM suppresses the transient peak overshoot in active power by 1.938% and 21.71% in DG-1 and DG-2 respectively. It can be observed that the suppression in DG-1 is negligible, as it operates at the maximum power point. The reactive power transient fluctuation is suppressed by 21.71% and 22.35% in both DG-1 and DG-2 respectively.

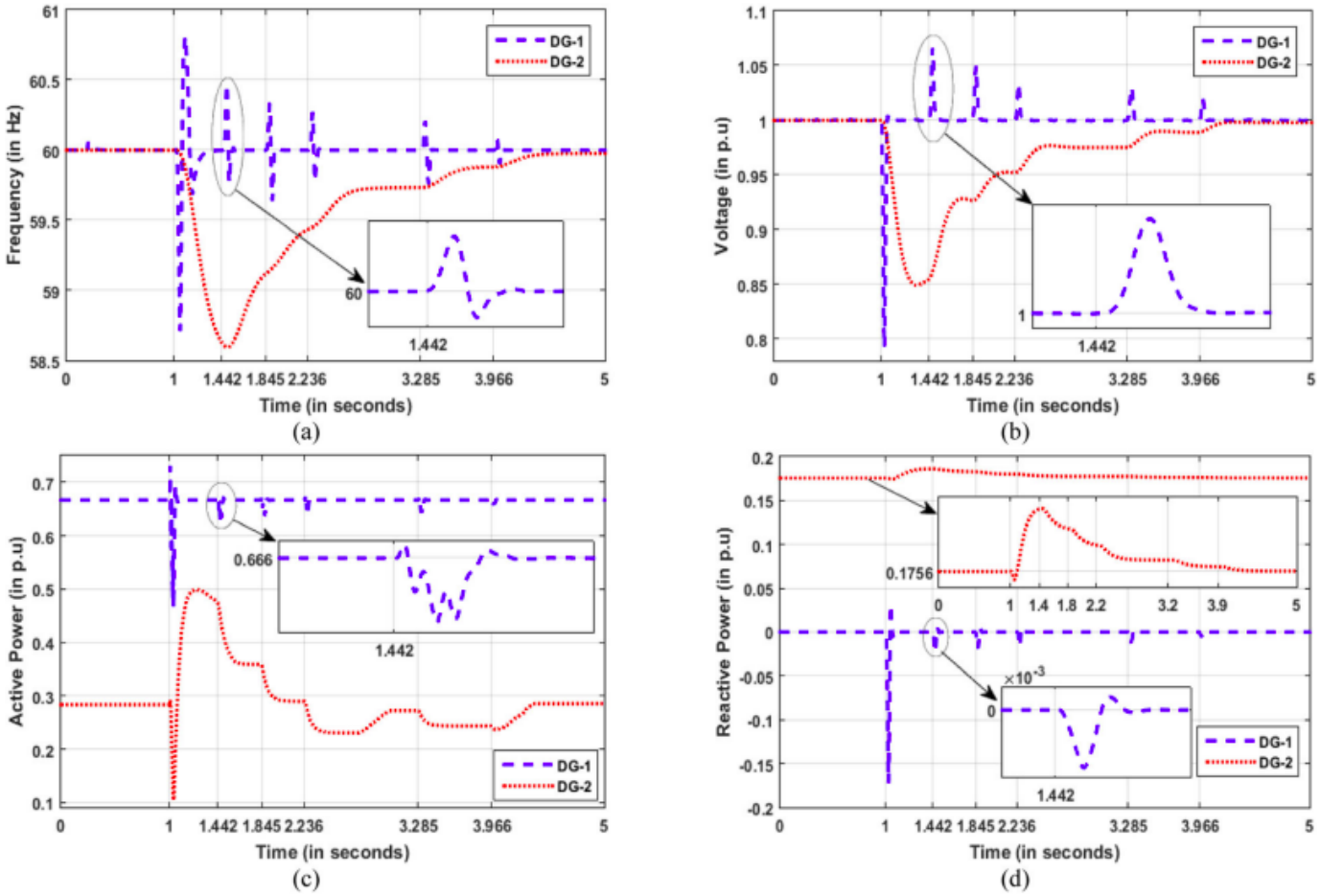


Fig. 12 DG performance during the load shedding strategy (a) Frequency, (b) Voltage, (c) Active power, (d) Reactive power

### *C. Case-3*

This case is stimulated at 0.86 power factor, to test the system performance under 30% of active power and 10% of reactive power overloading condition. The loads L11 to L16 are incorporated in the microgrid to simulate the overloading scenario. The case is designed such that it highlights the performance of power-sharing and load shedding strategy together. The islanding is assumed to have occurred at the time 1 s. The battery charges itself while present in grid-connected mode, and from the instance of islanding, the battery starts discharging as shown in Fig. 11a. The active power fed by the storage device is demonstrated in Fig. 11b. However, due to an extreme loading condition, the voltage and the frequency at the PCC tend to violate the threshold limit of frequency and voltage. The transient variations in voltage are compensated by the D-STAT COM as shown in Fig. 11c. The D-STATCOM also feeds an instantaneous reactive power into the system as illustrated in Fig. 11d. The load demand in the microgrid remains too high to make the system unstable. The frequency and the voltage of the DGs tending towards the instability can be analyzed from Fig. 12a and b respectively. Thus, the violation of the system parameter's limit at PCC triggers the load shedding strategy. The loads shed by the proposed shedding strategy are calculated using (14) and the approximate similar load values with the least priority are shed as shown in Table 2. The proposed load shedding strategy initializes the stage-I of the strategy and sheds the load in three iterations at time 1.4 s, 1.8 s, and 2.2 s. The effects of the load shedding on voltage and frequency are illustrated in Fig. 12a and b respectively. The MPP controlled DG-1 being an inertia-less power source

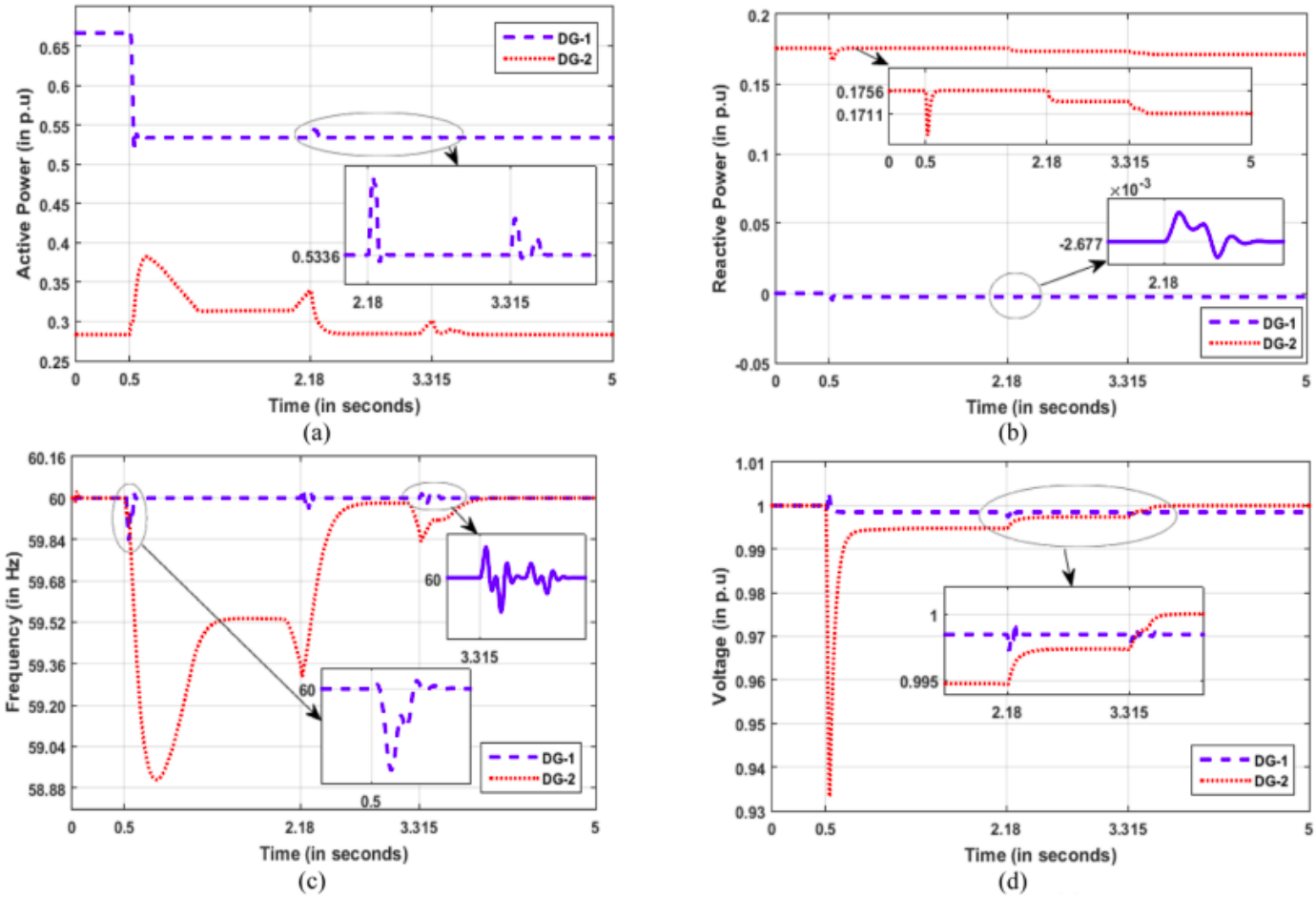


Fig. 13 System performance under reduced power generation (a) Frequency, (b) Voltage, (c) Active power, (d) Reactive power

responds with an insignificant time delay to the load shed. Whereas the DG-2 being a high inertia system shows a sluggish response and consumes a certain time to retain itself within the stability zone. The time consumed to retain the stability is compensated by the D-STATCOM present in the microgrid. The stage-I of the load shedding strategy tends the microgrid to attain the voltage and the frequency within the operating limits as shown in Fig. 12a and b. Further, when the df \ dt condition satisfies, the stage-II of the load shedding strategy is triggered. Though the system parameters are operating within the stability limit, but to achieve the system to be operating at a standard operating point, a small load is shed at a time about 3.2 s and the stage-III of the load shedding scheme sheds another small load at 3.9 s. The variations in active and reactive power generation of DG-1 and DG-2, corresponding to the load shed can be analyzed from Fig. 12c and Fig. 12d.

*D. Case-4*

In order to examine the proposed approach under a reduced power generation, the Case-4 is simulated. The power generation by DG-1 suddenly reduces from 100 kW to 80 kW of generation. The drop of 20 kW of power from DG-1 at time 0.5 s can be analyzed in Fig. 13. The battery operates in the discharge Stage-I instantly and feeds the maximum possible power of 15 kW into the system. The remaining 5 kW of power deficit is managed and fed by DG-2. At time 2 s, the battery attains 50% of SoC and tends to operate in the discharge stage-II of the battery as shown in Fig. 14a. Thus the battery reduces the rate of discharge and feeds the power of about 9 kW as in Fig. 14b. As a result, the surplus load demand of 11 kW is to be fed by DG-2 depicted in Fig. 13a. But from Fig. 13c and d it can be observed that the increase in power deficit leads the voltage and frequency towards instability. Therefore, the stage-II of the load shedding is triggered to shed the loads. So, a load is shed at 2.18 s. This shedding of load helps the voltage and the frequency of the DGs to attain the operating point. Further, as the battery reaches 30% of its SoC, two small loads are shed by the stage-III of the load shedding strategy after 3.3 s. These shedding lead the system towards the specified operating nominal value as shown in Fig. 13 and the amount and location where the load

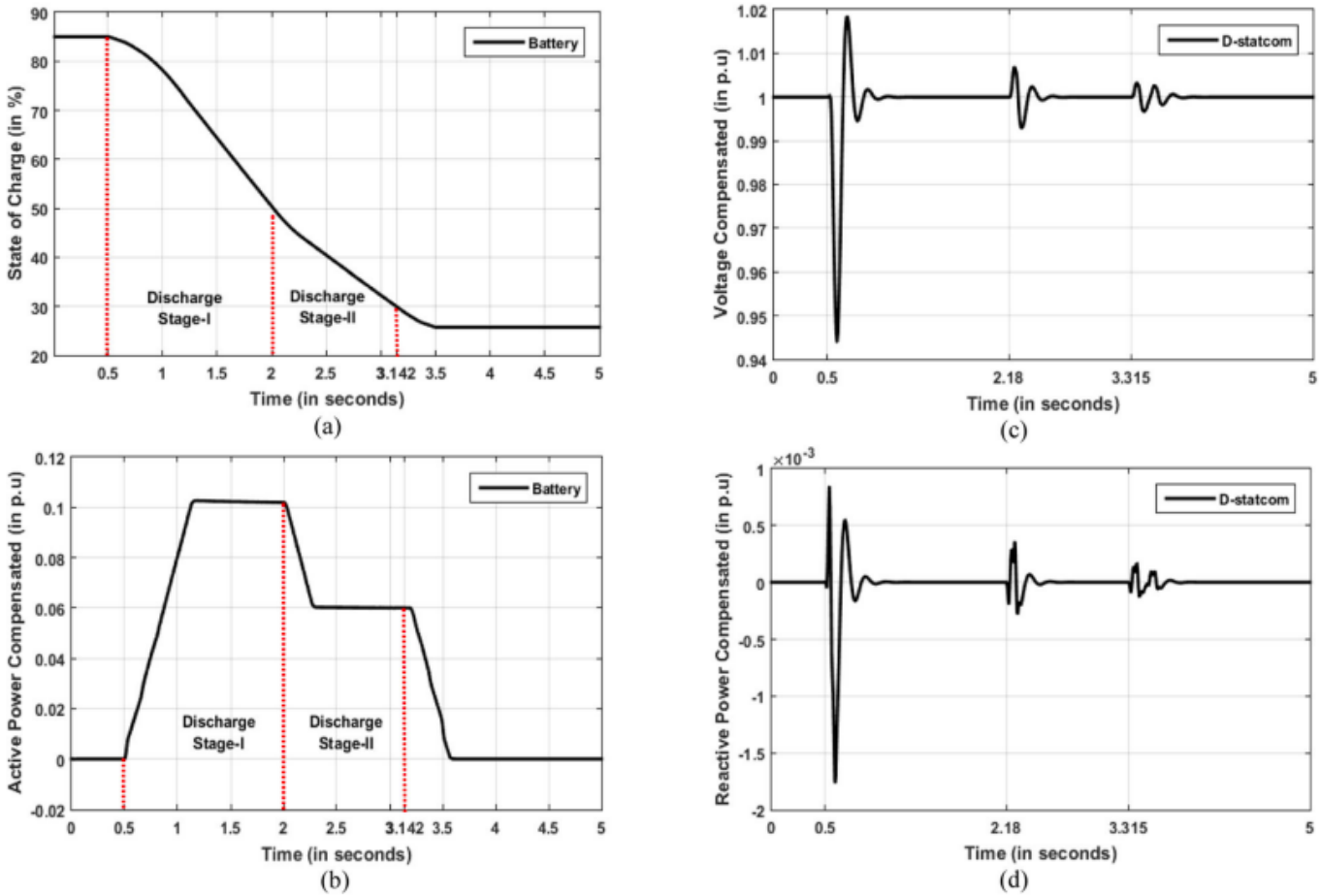


Fig. 14 Power fed by battery and D-STATCOM (a) Battery's state of charge (b) Active power compensated by battery (c) Voltage compensated by DSTATCOM (d) Reactive power compensated by DSTATCOM

## VI. Conclusion

The article aims to address the microgrid stability while operating in an autonomous mode of operation. The microgrid system undertaken integrates both inertia-less and high inertia power sources along with the storage system and the reactive power compensating device. The control strategy for each unit is elaborated in Section III of the manuscript. Each operating unit uses the P-f and Q-V power-sharing control strategy to maintain system stability. To deal with the worst-power deficit scenario, a load shedding strategy is proposed. The shedding strategy incorporates the microgrid storage system to prolong the loads for a certain time after attaining the frequency within the operational stability and limit. The D-STAT COM present in the system helps to avoid the instantaneous conflict of power-sharing between the two different types of inertial DG by compensating the voltage, and efficiently control the system stability for few cycles until the load shedding is initialized. The designed droop based load shedding strategy is only dependent on the system inertia. The strategy sheds load to control the reducing rateof-change-of-frequency. The precise shedding process is faster compared to the conventional schemes and confirms the difference between the operating frequency and nominal frequency to be approximately zero proving its robustness to act under a wide range of operating conditions.

## References

[1] Roy, N. K., Hossain, M. J., & Pota, H. R. (2011). Voltage profile improvement for distributed wind generation using D-STATCOM. In 2011 IEEE Power and Energy Society General Meeting (pp. 1–6). IEEE; Detroit.J. Clerk Maxwell, A Treatise on Electricity and Magnetism, 3rd ed., vol. 2. Oxford: Clarendon, 1892, pp.68–73.

[2] Divshali, P. H., Alimardani, A., Hosseinian, S. H., & Abedi, M. (2012). Decentralized cooperative control strategy of microsources for stabilizing autonomous VSC-based microgrids. IEEE Transactions on Power Systems, 27(4), 1949–1959.

[3] Paquette, A. D., Reno, M. J., Harley, R. G., & Divan, D. M. (2012). Transient load sharing between inverters and synchronous generators in islanded microgrids. In 2012 IEEE Energy Conversion Congress and Exposition (ECCE) (pp. 2735–2742). IEEE; Raleigh.

[4] Majumder, R., Ghosh, A., Ledwich, G., & Zare, F. (2009). Power sharing and stability enhancement of an autonomous microgrid with inertial and noninertial DGs with DSTATCOM. In 2009 International Conference on Power Systems (pp. 1–6). IEEE; Kharagpur.

[5] Raghami, A., Ameli, M. T., & Hamzeh, M. (2013). Primary and secondary frequency control in an autonomous microgrid supported by a loadshedding strategy. In 4th Annual International Power Electronics, Drive Systems and Technologies Conference (pp. 282–287). IEEE; Tehran.

[6] Bakar, N. N. A., Hassan, M. Y., Sulaima, M. F., Na'im Mohd Nasir, M., & Khamis, A. (2017). Microgrid and load shedding scheme during islanded mode: A review. Renewable and Sustainable Energy Reviews, 71, 161–169.

[7] Joe, A., & Krishna, S. (2015). An underfrequency load shedding scheme with minimal knowledge of system parameters. International Journal of Emerging Electric Power Systems, 16(1), 33–46.

[8] Rudez, U., & Mihalic, R. (2015). Predictive underfrequency load shedding scheme for islanded power systems with renewable generation. Electric Power Systems Research, 126, 21–28.

[9] El-Zonkoly, A. (2015). Application of smart grid specifications to overcome excessive load shedding in Alexandria, Egypt. Electric Power Systems Research, 124, 18–32.

[10] Lokay, H. E., & Burtnyk, V. (1968). Application of underfrequency relays for automatic load shedding. IEEE Transactions on Power Apparatus and Systems, 3, 776–783.

[11] Anderson, P. M., & Mirheydar, M. (1992). An adaptive method for setting underfrequency load shedding relays. IEEE Transactions on Power Systems, 7(2), 647–655.

[12] Delfino, B., Massucco, S., Morini, A., Scalera, P., & Silvestro, F. (2001). Implementation and comparison of different under frequency loadshedding schemes. In 2001 Power Engineering Society Summer Meeting. Conference Proceedings (Cat. No. 01CH37262) (Vol. 1, pp. 307–312). IEEE; Vancouver

[13] Rudez, U., & Mihalic, R. (2009). Analysis of underfrequency load shedding using a frequency gradient. IEEE Transactions on Power Delivery, 26(2), 565–575.

[14] Terzija, V. V. (2006). Adaptive underfrequency load shedding based on the magnitude of the disturbance estimation. IEEE Transactions on Power Systems, 21(3), 1260–1266

[15] Rudez, U., & Mihalic, R. (2011). A novel approach to underfrequency load shedding. Electric Power Systems Research, 81(2), 636–643

[16] Shekari, T., Aminifar, F., & Sanaye-Pasand, M. (2015). An analytical adaptive load shedding scheme against severe combinational disturbances. IEEE Transactions on Power Systems, 31(5), 4135–4143.

[17] Marzband, M., Moghaddam, M. M., Akorede, M. F., & Khomeyrani, G. (2016). Adaptive load shedding scheme for frequency stability enhancement in microgrids. Electric Power Systems Research, 140, 78–86.

[18] Ceja-Gomez, F., Qadri, S. S., & Galiana, F. D. (2012). Under-frequency load shedding via integer programming. IEEE Transactions on Power Systems, 27(3), 1387–1394

[19] Luan, W. P., Irving, M. R., & Daniel, J. S. (2002). Genetic algorithm for supply restoration and optimal load shedding in power system distribution networks. IEE Proceedings-Generation, Transmission and Distribution, 149(2), 145–151.

[20] Chuvychin, V., & Petrichenko, R. (2013). Development of smart underfrequency load shedding system. Journal of Electrical Engineering, 64(2), 123–127.

[21] Delille, G., Francois, B., & Malarange, G. (2012). Dynamic frequency control support by energy storage to reduce the impact of wind and solar generation on isolated power system's inertia. IEEE Transactions on Sustainable Energy, 3(4), 931–939.

[22] Zhang, L., Liu, Y., & Crow, M. L. (2005, 2005). Coordination of UFLS and UFGC by application of D-SMES. In IEEE Power Engineering Society General Meeting (pp. 1064–1070). IEEE; San Francisco.